




 Cite this: *RSC Adv.*, 2023, **13**, 8630

# DBU-intercalated $\gamma$ -titanium phosphate as a latent thermal catalyst in the reaction of glycidyl phenyl ether (GPE) and hexahydro-4-methylphthalic anhydride (MHHPA)

 Ayumi Fujiwara,<sup>a</sup> Hiroshi Furuya,<sup>a</sup> Shekh Md. Mamun Kabir,<sup>ac</sup> Motohiro Shizuma,<sup>b</sup> Atsushi Ohtaka <sup>a</sup> and Osamu Shimomura <sup>\*a</sup>

The capabilities and performance of  $\gamma$ -titanium phosphate ( $\gamma$ -TiP) with 1,8-diazabicyclo[5.4.0]undec-7-ene (DBU) as a latent thermal catalyst were investigated by the copolymerization of glycidyl phenyl ether (GPE) and hexahydro-4-methylphthalic anhydride (MHHPA) at different temperatures for a period of one hour. Polymerization was not observed until the reactants were heated to 100 °C. Upon increasing the temperature to 120 °C, the conversion in the presence of  $\gamma$ -TiP·DBU as a catalyst showed 98% conversion in 1 h. The thermal stability of GPE and MHHPA reacted in the presence of  $\gamma$ -TiP·DBU at 40 °C for 144 h resulted in less than 7% conversion of GPE. The conversion of GPE did not show a significant increase at 40 °C.

Received 24th December 2022

Accepted 1st March 2023

DOI: 10.1039/d2ra08209h

[rsc.li/rsc-advances](https://rsc.li/rsc-advances)

## 1. Introduction

The nanolayered structures of  $\alpha$ -M(HPO<sub>4</sub>)<sub>2</sub>·H<sub>2</sub>O and  $\gamma$ -M(HPO<sub>4</sub>)<sub>2</sub>·2H<sub>2</sub>O (M = Ti, Zr, Sn, Ge, Pb, *etc.*) have attracted increasing attention in recent decades due to their ion exchange capacity and application in drug delivery.<sup>1–5</sup>  $\alpha$ -Zirconium phosphate ( $\alpha$ -ZrP) with a small metal cation or interlaced with an amine can provide a larger interlayer distance for the further uptake of species such as a metal cation with a large ionic radius, an alcohol/glycol, and a quaternary ammonium cation, which can be considered as a catalyst and reinforcement of polymers.<sup>6–10</sup> Thermal latent catalysts and initiators are highly attractive for use in chemical industries such as adhesives, paints, and molding materials. Salt-type and non-salt-type thermal latent initiators such as sulfonium salt, phosphonium salt, pyridinium salt, *N*-heterocyclic carbene, aminimide, phosphoramidates, *O,O*-di-*t*-butyl phenyl phosphonate and phosphonic amide ester are used in polymerization.<sup>11</sup> We have already reported that primary alkylamines intercalated with  $\alpha$ -ZrP can serve as latent thermal initiators in the reaction of glycidyl phenyl ether (GPE)<sup>12</sup> and that 1,4-diazabicyclo (2,2,2) octane (DABCO) and 1,8-diazabicyclo (5,4,0) undec-7-ene (DBU) are intercalation compounds with  $\alpha$ -ZrP.<sup>13</sup> Furthermore, we examined the performances of some imidazoles intercalated

with  $\alpha$ -ZrP as thermal latent initiators.<sup>14,15</sup>  $\alpha$ -ZrP·DABCO and  $\alpha$ -ZrP·DBU show good performance as latent thermal catalysts in the reaction of GPE and hexahydro-4-methylphthalic anhydride (MHHPA). However,  $\alpha$ -ZrP-intercalated DBU needs a higher temperature for the reaction of GPE and MHHPA. Therefore, researchers mainly focused on developing a highly active latent catalyst to avoid the need for high-temperature curing.  $\gamma$ -Insoluble acid salts are tetravalent metals that can be obtained with a different layered structure, first obtained by Clearfield.<sup>1</sup> Furthermore, the layers of  $\gamma$ -titanium phosphate ( $\gamma$ -TiP) and  $\alpha$ -ZrP are packed at different interlayer distances, and hence, they show different ion exchange properties.<sup>1</sup> The interlayer distance of  $\alpha$ -Zr (HPO<sub>4</sub>)<sub>2</sub>·H<sub>2</sub>O (7.6 Å) and  $\gamma$ -Ti (HPO<sub>4</sub>)<sub>2</sub>·2H<sub>2</sub>O (11.6 Å) has been reported.<sup>16</sup> The wide interlayer distance of  $\gamma$ -TiP might show high reactivity compared with  $\alpha$ -ZrP.  $\gamma$ -TiP can be easily prepared by converting amorphous TiP with the treatment of concentrated H<sub>3</sub>PO<sub>4</sub> at 225 °C for 48 h.<sup>17</sup>

In the present study, we report that  $\gamma$ -TiP intercalated with DBU was synthesized. This material could be a cheaper and alternative thermal latent catalyst than  $\alpha$ -ZrP for the reaction of GPE and MHHPA. Therefore, the enhancement effects of  $\gamma$ -TiP as a potential thermal latent catalyst on the acceleration of the reaction between GPE and MHHPA were extensively studied.

## 2. Results and discussion

The intercalation of DBU into the layers of  $\gamma$ -TiP was carried out by a similar procedure of intercalation into  $\alpha$ -ZrP. The mixture of DBU and  $\gamma$ -TiP in methanol was stirred at ambient temperature for 24 h. After the reaction, the intercalation compound

<sup>a</sup>Department of Applied Chemistry, Osaka Institute of Technology, 5-16-1 Omiya, Ashahi-ku, Osaka 535-8585, Japan. E-mail: osamu.shimomura@oit.ac.jp

<sup>b</sup>Osaka Research Institute of Industrial Science and Technology, 1-6-50 Morinomiya, Joto-ku, Osaka 536-8553, Japan

<sup>c</sup>Department of Wet Process Engineering, Bangladesh University of Textiles, Tejgaon, Dhaka-1208, Bangladesh



was recovered by centrifugation and dried under vacuum. The ratio of C, H, and N of the product was 14.81%, 2.60%, and 3.84%, and the composition was  $\text{Ti}(\text{HPO}_4)_2 \cdot 0.40\text{DBU}$ , as determined by elemental analysis. The interlayer distance of the intercalation compound of  $\gamma\text{-TiP} \cdot \text{DBU}$  was 19.6 Å ( $2\theta = 4.5^\circ$ ) expanded from 11.5 Å ( $2\theta = 7.7^\circ$ ) of pristine  $\gamma\text{-TiP}$  estimated by XRD patterns, as shown in Fig. 1(a) and (b). The thermal properties of  $\gamma\text{-TiP} \cdot \text{DBU}$  were examined by TG and DSC, as shown in Fig. 2 and 3. Pristine  $\gamma\text{-TiP}$  loses two molecules of crystal water from 50 to 100 °C.<sup>16</sup> As shown in Fig. 2,  $\gamma\text{-TiP} \cdot \text{DBU}$  gradually lost the weight in the first step until 220 °C (6.5% of weight loss). The DSC curve up to 220 °C shows two endothermic peaks, and the peak temperatures are 104.4 °C and 193.3 °C, as shown in Fig. 2. The third endothermic peak was observed at 423.4 °C from 300 °C to 550 °C. Assuming that the weight loss of 20.8% from 25 °C to 590 °C was attributed to that of DBU, the compositional formula was calculated as  $\text{Ti}(\text{HPO}_4)_2 \cdot (\text{C}_9\text{H}_{16}\text{N}_2)_{0.41}$ . From the compositional formula calculated from the elemental analysis, the composition was  $\text{Ti}(\text{HPO}_4)_2 \cdot (\text{C}_9\text{H}_{16}\text{N}_2)_{0.40}$ . The decreasing weight was in good accordance with the deintercalation of DBU. It could be explained that  $\gamma\text{-TiP}$  shows a two-step titration curve with a NaOH–NaCl solution.<sup>1</sup> At least two peaks would be indicated in the DSC curve. The reaction of GPE–MHHPA with  $\gamma\text{-TiP} \cdot \text{DBU}$ , as shown in Scheme 1, was carried out at 120 °C for 4 h, the polymer products obtained were washed out with THF and the residue of  $\gamma\text{-TiP} \cdot \text{DBU}$  ( $\gamma\text{-TiP} \cdot \text{DBU} \cdot \text{RXN}$ ) was recovered. The interlayer distance of  $\gamma\text{-TiP} \cdot \text{DBU} \cdot \text{RXN}$  was 25.7 Å ( $2\theta = 3.4^\circ$ ) expanded from  $\gamma\text{-TiP} \cdot \text{DBU}$ , as shown in Fig. 1(c).

The expansion of the basal distance and an increase in the C content were recognized. The  $^{13}\text{C}$  CPMAS NMR spectrum of  $\gamma\text{-TiP} \cdot \text{DBU}$  and  $\gamma\text{-TiP} \cdot \text{DBU} \cdot \text{RXN}$  are shown in Fig. 4. In the  $^{13}\text{C}$  CPMAS NMR spectrum, the aromatic carbons, methine, and methylene groups derived from GPE are shown in Fig. 4(b). The copolymer of GPE–MHHPA, carbonyl carbon, must be observed at  $\delta$  175. In the  $^{13}\text{C}$  CPMAS NMR of  $\gamma\text{-TiP} \cdot \text{DBU} \cdot \text{RXN}$ , carbonyl carbon was not observed at  $\delta$  175. A similar result was observed with  $\alpha\text{-ZrP}$  imidazoles.<sup>14</sup> The C, H, and N ratio of the product by elemental analysis was 33.03 : 3.46 : 1.28. Based on the result, the reaction products exist in the interlayer of  $\gamma\text{-TiP} \cdot \text{DBU}$ , and the composition was estimated as  $\text{Ti}(\text{HPO}_4)_2 \cdot \text{DBU}_{0.20} \cdot (\text{GPE})_{1.15}$ . At 50%, the interlayer of DBU remained after the reaction of GPE–MHHPA. We have already reported using  $\alpha\text{-ZrP} \cdot \text{DBU}$  that the remaining DBU was 20%.<sup>13</sup> The deintercalated DBU initiated the copolymerization of GPE and MHHPA. The deintercalation ratio would be affected by the reactivity of GPE–MHHPA. The FT-IR spectra of  $\alpha\text{-ZrP} \cdot \text{DBU}$  and  $\alpha\text{-ZrP} \cdot \text{DBU} \cdot \text{RXN}$  are shown in Fig. 5(b) and (c). The peak due to DBU ( $\nu$  C=N) and  $\alpha\text{-ZrP}$  ( $\nu$  P–O) was detected at 1650 and 983  $\text{cm}^{-1}$  in Fig. 5(b). The aromatics ( $\nu$  C–C at 1600 and 1548  $\text{cm}^{-1}$ ) and ether groups ( $\nu$  C–O–C at 1230  $\text{cm}^{-1}$ ) in the products of GPE are observed in Fig. 5(c).

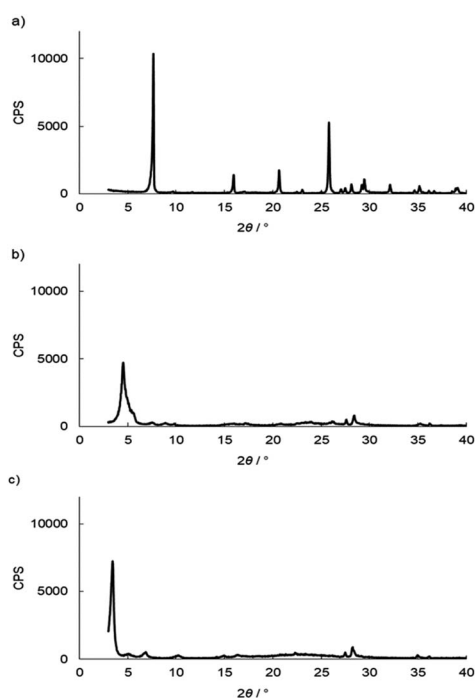


Fig. 1 XRD patterns of (a) pristine  $\gamma\text{-TiP}$ , (b)  $\gamma\text{-TiP} \cdot \text{DBU}$ , and (c)  $\gamma\text{-TiP} \cdot \text{DBU} \cdot \text{RXN}$ .

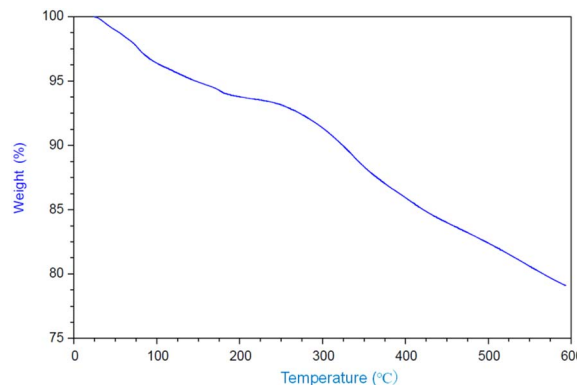


Fig. 2 TGA curve of  $\gamma\text{-TiP} \cdot \text{DBU}$ .

The estimation of the catalytic activity of  $\gamma\text{-TiP} \cdot \text{DBU}$  and the copolymerization of GPE and MHHPA was carried out as shown in Fig. 6. The reaction of GPE–MHHPA with  $\alpha\text{-ZrP} \cdot \text{DBU}$  has already been reported.<sup>13</sup> In comparison to GPE conversions at 100 °C, the greatest difference between the conversions was 68% and 35% with  $\gamma\text{-TiP} \cdot \text{DBU}$  and  $\alpha\text{-ZrP} \cdot \text{DBU}$ , as determined by the  $^1\text{H}$ -NMR spectra. Conversions at 120 °C were 98% and

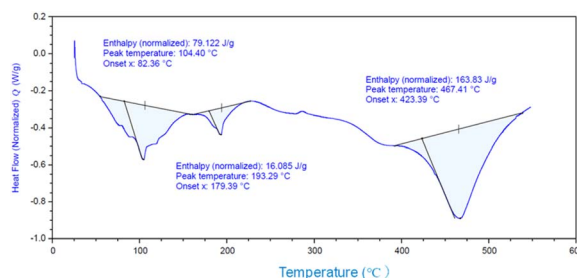
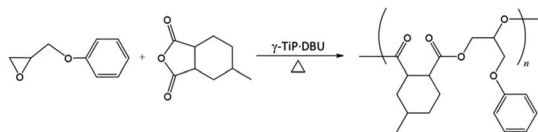
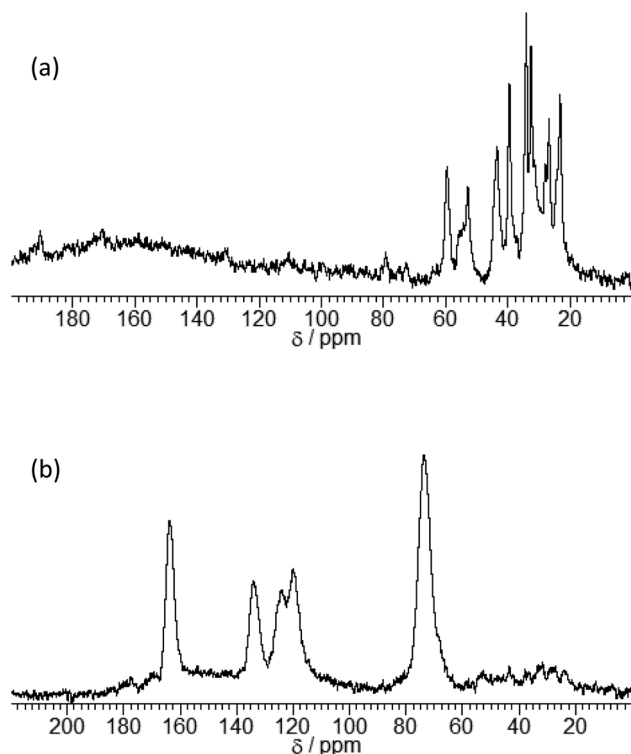


Fig. 3 DSC curve of  $\gamma\text{-TiP} \cdot \text{DBU}$ .





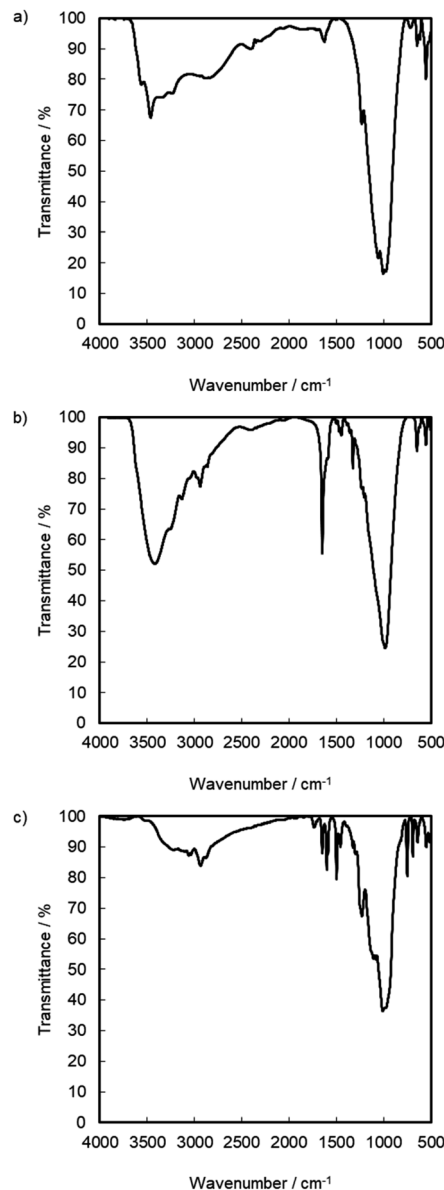
Scheme 1 Synthesis of poly(GPE-co-MHHPA).

Fig. 4  $^{13}\text{C}$ -NMR spectra of (a)  $\gamma$ -TiP-DBU and (b)  $\gamma$ -TiP-DBU-RXN.

86% with  $\gamma$ -TiP-DBU and  $\alpha$ -ZrP-DBU. The reaction with  $\gamma$ -TiP-DBU quantitatively proceeded at 120 °C and  $\gamma$ -TiP-DBU was higher reactivity at the same reaction temperature.

The copolymerization of GPE-MHHPA and homopolymerization of GPE might occur simultaneously. The conversion of MHHPA was confirmed by the integral ratio at different temperatures for 1 h (Fig. 7). However,  $\gamma$ -TiP-DBU has shown a conversion of 67% at 100 °C and increased the conversion rate by 96% at 120 °C. It can be explained that the conversion of GPEs was in good accordance with MHHPA and  $\gamma$ -TiP-DBU accelerates the reaction rate more than  $\alpha$ -ZrP-DBU. The reaction with  $\gamma$ -TiP-DBU quantitatively proceeded at 120 °C and  $\gamma$ -TiP-DBU has higher reactivity at the same reaction temperature. It might be explained that  $\gamma$ -TiP shows a two-step titration curve with the NaOH-NaCl solution. Under a similar condition,  $\alpha$ -ZrP shows a one-step titration curve, as reported in the literature.<sup>1</sup> It can affect the first step of deintercalation of DBU from the interlayer of  $\gamma$ -TiP.

The conversion of GPE after 1 h as a function of the content of DBU in  $\gamma$ -TiP-DBU during polymerization is shown in Fig. 8. When the mole concentration of DBU increased, and the

Fig. 5 FT-IR spectrum of (a) pristine  $\gamma$ -TiP, (b)  $\gamma$ -TiP-DBU, and (c)  $\gamma$ -TiP-DBU-RXN.

conversion rate also increased. The comparison of the conversions of GPE was 95% by using 2 mol% of  $\gamma$ -TiP-DBU. There is also a very important observation in the presence of  $\gamma$ -TiP-DBU; the use of more than 2 mol%  $\gamma$ -TiP-DBU resulted in copolymerization of GPE and MHHPA.

The conversion values for GPE with 3 mol% of  $\gamma$ -TiP-DBU at 120 °C for 0–60 min are displayed in Fig. 9. It can be seen that the conversion values increased with the increasing reaction time and reached 94% after 30 min. It is clear that the polymerization reaction proceeds within a short period after 30 min under specific conditions. In addition, by extending the time period, the conversion rate also increased and reached 97% conversion for 45 min.

The performance of the latent thermal initiator depends on the high curing capacity at the desired temperature and higher



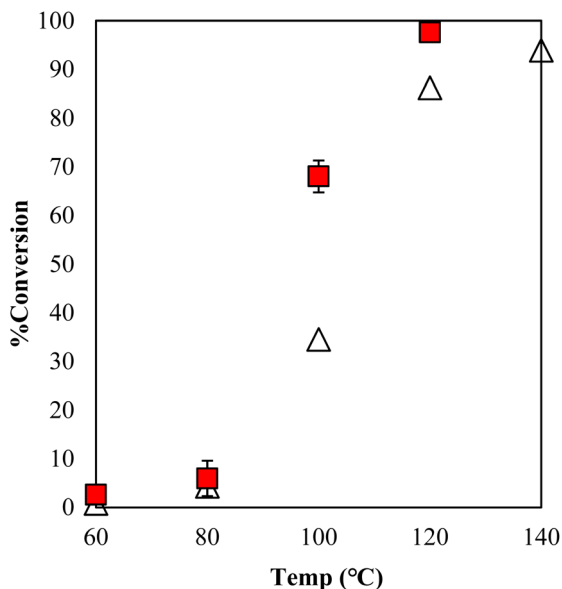


Fig. 6 Conversion of GPE after 1 h as a function of temperature during polymerization with  $\gamma$ -TiP·DBU (■) and  $\alpha$ -ZrP·DBU ( $\Delta$ ).<sup>15</sup>

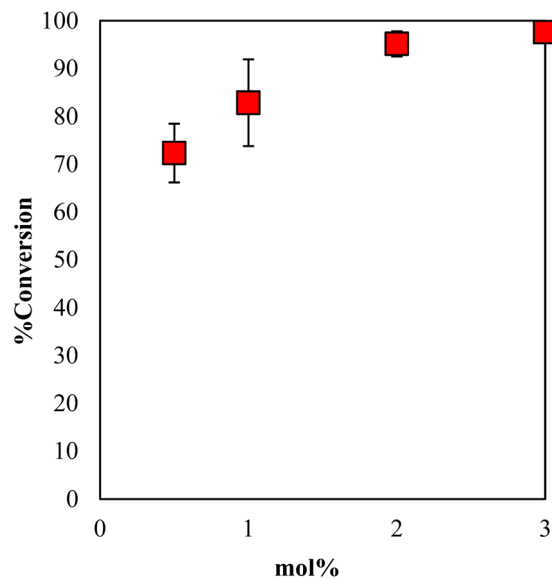


Fig. 8 Conversion of GPE after 1 h as a function of the content of DBU in  $\gamma$ -TiP·DBU during polymerization at 120 °C.

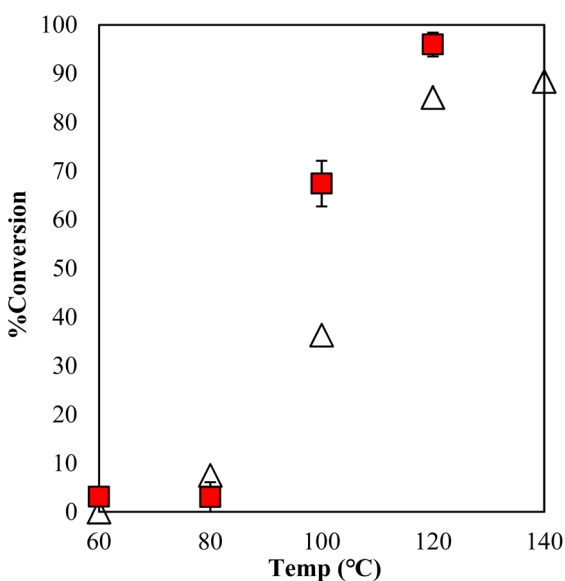


Fig. 7 Conversion of MHHPA after 1 h as a function of temperature during polymerization with  $\gamma$ -TiP·DBU (■) and  $\alpha$ -ZrP·DBU ( $\Delta$ ).<sup>15</sup>

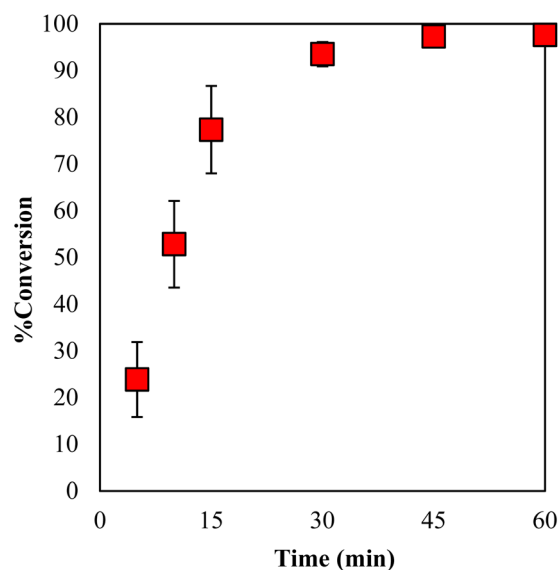


Fig. 9 Conversion of GPE as a function of time during polymerization with  $\gamma$ -TiP·DBU at 120 °C.

storage stability under the recommended storage conditions. The evaluation of the performance of storage stability is mainly based on the conversion of GPE as a function of time during polymerization with  $\gamma$ -TiP·DBU and  $\alpha$ -ZrP·DBU at 40 °C, as presented in Fig. 10. The conversion did not show a significant increase, and the conversion was 5% for 144 h.

## 3. Experimental section

### 3.1. Materials

Ti(HPO<sub>4</sub>)<sub>2</sub>·2H<sub>2</sub>O was purchased from Rasa Industries Ltd (Japan); GPE, DBU, and MHHPA from Tokyo Chemical

Industries, Co., Ltd (Japan). Solvents were used as received without further purification.

### 3.2. Measurements

X-ray diffraction (XRD) patterns were acquired using a Rigaku RINT2200 (Japan) with Cu K $\alpha$  radiation over a scan range of 3–40° at a rate of 2° min<sup>-1</sup>. NMR spectra in solutions were recorded using a Varian Unity-300 spectrometer (Palo Alto, CA, USA) with tetramethylsilane (TMS) as an internal standard. The DBU contents in the intercalation compounds of  $\gamma$ -TiP were measured using a PerkinElmer 2400II analyzer (Waltham, MA,



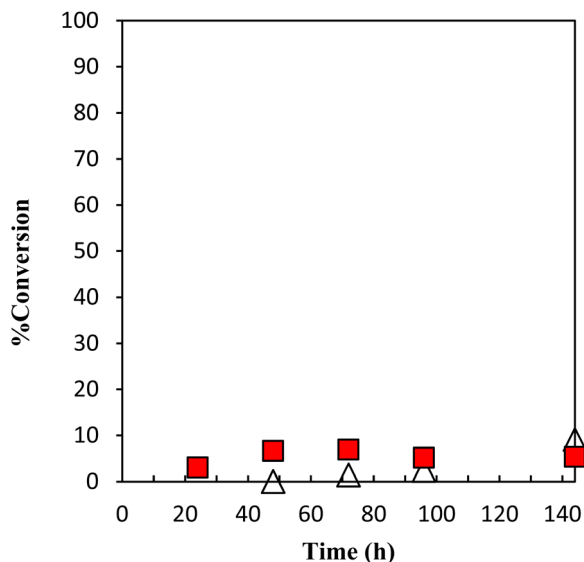


Fig. 10 Conversion of GPE as a function of time during polymerization with  $\gamma$ -TiP·DBU at 40 °C.  $\gamma$ -TiP·DBU (■) and  $\alpha$ -ZrP·DBU (Δ).<sup>13</sup>

USA). The <sup>13</sup>C CPMAS NMR spectra were recorded using a JEOL ECA-600 NMR spectrometer (Tokyo, Japan). Thermogravimetric (TG) analysis was carried out using a TA instrument TGA-550 at a heating rate of 10 °C min<sup>-1</sup> under nitrogen. Differential scanning calorimetry (DSC) was carried out using a TA instrument DSC250 at a heating rate of 10 °C min<sup>-1</sup> under nitrogen.

### 3.3. Preparation of DBU-intercalated $\gamma$ -TiP ( $\gamma$ -TiP·DBU)

The intercalation of DBU into the layers of  $\text{Ti}(\text{HPO}_4)_2 \cdot 2\text{H}_2\text{O}$  ( $\gamma$ -TiP) was carried out following a similar procedure for  $\alpha$ -Zirconium phosphate.  $\gamma$ -TiP (4.98 g) and DBU (8.38 g) were added to methanol (75.2 mL). The reaction mixture was agitated at ambient temperature for 24 h before the product was collected by centrifugation and washed 3 times with methanol. The resulting residue was dried under vacuum. The ratio of C, H, and N in the product was 14.81 : 2.60 : 3.84, and the composition was  $\text{TiP}(\text{HPO}_4)_2 \cdot 0.40\text{DBU}$ , as determined by elemental analysis.

### 3.4. Typical polymerization procedure

A mixture of GPE (150 mg, 1.0 mmol), MHHPA (166 mg, 0.99 mmol), and  $\gamma$ -TiP·DBU (22.1 mg, 0.075 mmol, DBU content: 0.030 mmol) was heated at 100 °C for 1 h. A small aliquot of the reaction mixture was dissolved in  $\text{CDCl}_3$ , and its <sup>1</sup>H-NMR spectrum was recorded to determine the extent of conversion of GPE.

### 3.5. Recovery of $\gamma$ -TiP·DBU after the reaction with GPE and MHHPA ( $\gamma$ -TiP·DBU-RXN)

A mixture of GPE (7.51 g, 50.0 mmol), MHHPA (8.41 g, 50.0 mmol), and  $\gamma$ -TiP·DBU (535 mg, 1.82 mmol, DBU content: 0.73 mmol) was heated at 120 °C for 4 h. After the reaction, tetrahydrofuran (THF) was added to the mixture. The solution was

filtered and the residue,  $\gamma$ -TiP·DBU-RXN, was rinsed, dried under vacuum, and analyzed by XRD and <sup>13</sup>C CPMAS NMR spectra. The C, H, and N ratio in  $\gamma$ -TiP·DBU-RXN was 33.03 : 3.46 : 1.28.

## 4. Conclusions

A temperature-dependent latent thermal catalyst  $\gamma$ -titanium phosphate ( $\gamma$ -TiP) intercalated with DBU has been introduced in the reaction of glycidyl phenyl ether (GPE) and hexahydro-4-methylphthalic anhydride (MHHPA) and compared with  $\alpha$ -ZrP-intercalated DBU. The interlayer distance of the intercalation compound of  $\gamma$ -TiP·DBU has shown 19.6 Å expanded from 11.5 Å of pristine  $\gamma$ -TiP. In the reaction with GPE and MHHPA at 120 °C for 1 h, the conversion value of GPE has been reached at 99% by  $\gamma$ -TiP·DBU. In addition, the conversion of MHHPAs was in good accordance with the conversion of GPEs. The conversion values of GPE increased with the increasing reaction time and reached 96% after 30 min and 98% after 45 min, by the reaction as a function of time during polymerization with  $\gamma$ -TiP·DBU. The latent thermal catalyst  $\gamma$ -TiP·DBU showed good stability under typical storage conditions (144 h at 40 °C), and was highly reactive with GPE and MHHPA. Thus, it can be suggested that  $\gamma$ -TiP·DBU could be a good alternative as a latent thermal initiating system in curing epoxy resins.

## Author contributions

Osamu Shimomura conceived, designed, and wrote the article; Ayumi Fujiwara, Hiroshi Furuya, and Motohiro Shizuma performed the experiments; Shekh Md. Mamun Kabir and Atsushi Ohtaka contributed to a helpful discussion.

## Conflicts of interest

The authors declare no conflict of interest.

## Acknowledgements

We thank Common Facilities Division of Office for Research Initiative and Development, Nagasaki University for elemental analyses.

## Notes and references

- 1 *Inorganic Ion Exchange Materials*, ed. A. Clearfield, CRC Press, Inc., Boca Raton, 1982.
- 2 I. H. Chowdhury and M. K. Naskar, *RSC Adv.*, 2016, **6**, 67136–67142.
- 3 Y. Zhang, X. Chen and W. Yang, *Sens. Actuators, B*, 2008, **130**, 682–688.
- 4 J. González-Villegas, Y. Kan, V. I. Bakhmutov, A. García-Vargas, M. Martínez, A. Clearfield and J. L. Colón, *Inorg. Chim. Acta*, 2017, **468**, 270–279.
- 5 H. Ueoka, O. Shimomura, M. Pica, A. Donnadio and R. Nomura, *Colloid Interface Sci. Commun.*, 2019, **28**, 29–33.



- 6 H. Ding, S. T. Khan, K. N. Aguirre, R. S. Camarda, J. B. Gafney, A. Clearfield and L. Sun, *Inorg. Chem.*, 2020, **59**, 7822–7829.
- 7 J. Baker, F. Xia, Z. Zhu, X. Zhang and H. J. Sue, *Langmuir*, 2020, **36**, 11948–11956.
- 8 Y. Zhou, I. Noshadi, H. Ding, J. Liu, R. S. Parnas, A. Clearfield, M. Xiao, Y. Meng and L. Sun, *Catalysts*, 2018, **8**, 17–18.
- 9 Y. Zhou, R. Huang, F. Ding, A. D. Brittain, J. Liu, M. Zhang, M. Xiao, Y. Meng and L. Sun, *ACS Appl. Mater. Interfaces*, 2014, **6**, 7417–7425.
- 10 W. J. Boo, L. Sun, G. L. Warren, E. Moghbelli, H. Pham, A. Clearfield and H. J. Sue, *Polymer*, 2007, **48**, 1075–1082.
- 11 J. Chen, N. Chu, M. Zhao, F. L. Jin and S. J. Park, *J. Appl. Polym. Sci.*, 2020, 137.
- 12 O. Shimomura, K. Maeno, A. Ohtaka, S. Yamaguchi, J. Ichihara, K. Sakamoto and R. Nomura, *J. Polym. Sci., Part A: Polym. Chem.*, 2014, **52**, 1854–1861.
- 13 O. Shimomura, T. Nishisako, S. Yamaguchi, J. Ichihara, M. Kirino, A. Ohtaka and R. Nomura, *J. Mol. Catal. A: Chem.*, 2016, **411**, 230–238.
- 14 O. Shimomura, K. Tokizane, T. Nishisako, S. Yamaguchi, J. Ichihara, M. Kirino, A. Ohtaka and R. Nomura, *Catalysts*, 2017, **7**, 172.
- 15 O. Shimomura, S. Sasaki, K. Kume, S. Kawano, M. Shizuma, A. Ohtaka and R. Nomura, *Catalysts*, 2019, **9**, 69.
- 16 A. M. K. Andersen and P. Norby, *Inorg. Chem.*, 1998, **37**, 4313–4320.
- 17 W. Zhang, R. Koivula, E. Wiikinkoski, J. Xu, S. Hietala, J. Lehto and R. Harjula, *ACS Sustainable Chem. Eng.*, 2017, **5**, 3103–3114.

